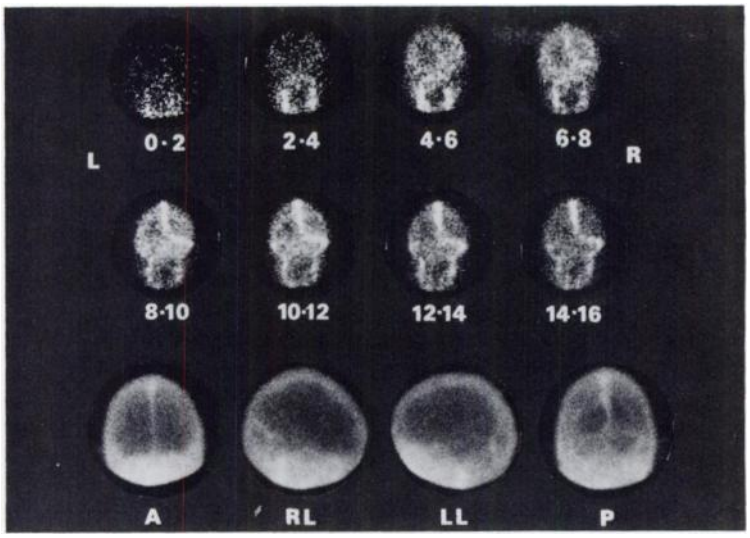

FIG. 1. Upper two rows show posterior dynamic perfusion studies. Left parieto-occipital region shows region of decreased perfusion throughout arterial, capillary, and venous phases. Numbers denote time ranges in seconds. Bottom row shows static brain images in anterior (A), right lateral (RL), left lateral (LL), and posterior (P) projections. These 2-hr postinjection scintigrams were interpreted as normal.

FIG. 2. Cranial computed tomography depicting left occipitoparietal extradural hematoma.

shaped area of increased density consistent with acutely extravasated blood in the left occipitoparietal region. The appearance was typical of an extradural hematoma. Retrograde right brachial, direct left carotid, and direct left brachial arteriograms were normal. A craniotomy performed the following day revealed a 40-cc left occipitoparietal subacute extradural hematoma. A review of the literature failed to uncover any previous report of extradural hemorrhage that produced a focal defect on the nuclear angiogram (*4–12*).

JOHN F. ROCKETT
EDWARD S. KAPLAN
M. MOINUDDIN
Baptist Memorial Hospital
Memphis, Tennessee

REFERENCES

1. LIN MS: Diagnostic scintigraphic sign in epidural hematoma at the vertex: Case report. *J Nucl Med* 17: 972–974, 1976

2. BUOZAS DJ, BARRETT IR, MISHKIN FS: Diagnosis of epidural hematoma by brain scan and perfusion study: Case report. *J Nucl Med* 17: 975–976, 1976

3. ZILKHA A, IRWIN GAL: The rim sign in epidural hematoma: Case report. *J Nucl Med* 17: 977–979, 1976

4. RONAI PM: Epilogue on extradural hematoma. *J Nucl Med* 17: 986–987, 1976

5. TER BRUGGE KG, MEINDOK H: Rim sign in brain scintigraphy of epidural hematoma. *J Nucl Med* 14: 709–710, 1973

6. FEINDEL W, ROVIT RL, STEPHENS-NEWSHAM L: Localization of intracranial vascular lesions by radioactive isotopes and an automatic contour brain scanner. *J Neurosurg* 18: 811–821, 1961

7. KRAMER S, ROVIT RL: The value of ^{203}Hg brain scans in patients with intracranial hematomas. *Radiology* 83: 902–909, 1964

8. GILSON AJ, GARGANO FP: Correlation of brain scans and angiography in intracranial trauma. *Am J Roentgenol Radium Ther Nucl Med* 94: 819–827, 1965

9. CIRIC IS, QUINN JL, BUCY PC: Mercury 197 and technetium 99m brain scans in the diagnosis of non-neoplastic intracranial lesions. *J Neurosurg* 27: 119–125, 1967

10. MORLEY JB, LANGFORD KH: Abnormal brain scan with subacute extradural haematomas. *J Neurol Neurosurg Psychiatry* 33: 679–686, 1970

11. VON ORTNER WD, KOLLAR WAF: Infratentorielle epidurale hamatome. *Munch Med Wochenschr* 114: 448–450, 1972

12. JAIN KK, SCHOBER B: Diagnosis of extradural hematoma by brain scan. *Can Med Assoc J* 107: 218–219, 1972

13. SILBERSTEIN EB: Epidural hematoma with decreased radionuclide uptake. *J Nucl Med* 15: 712–713, 1974

Anger Scintillation Camera as Whole-Body Counter for Quantitation and Visualization of Radionuclide Retention

We have noted with interest reports by Hofeldt and Verdon (*1,2*) published in this journal. Both reports dealt with the use of the Anger scintillation camera with an uncollimated crystal and "Chair" geometry as a whole-body counter. Currently these authors are evaluating the usefulness of this method to determine the extent of residual postoperative thyroid tissue in patients undergoing surgery for cancer of the thyroid.

With regard to these studies we would like to mention that as early as 1968 we reported our experience (*3*) with the Anger camera as a whole-body counter in followup studies of thyroid cancer patients. This work was also published later in detail (*4*). Our camera* used pinhole collimation. Simultaneous quantitation and visualization of the retained

activity is achieved by the use of a test dose of 1–5 mCi of ^{131}I. The patient is viewed in the supine position, 75 cm from the camera, and measurements are carried out immediately after the receipt of the test dose and again 72 hr later. The collimator's axis is aimed at the patient's xyphoid, excluding the lower extremities from the measurement. Retention, expressed as percentage of the dose, is calculated from the patient's 100% value, and the 72-hr measurement is corrected for efficiency variations by comparison with a dose aliquot. Errors due to counting geometry and redistribution are found to be tolerable. Results obtained with this technique in hypothyroid patients, without residual thyroid tissue, correspond well with data obtained with conventional whole-body counters (*5*).

For many years our technique of quantitating and visualizing iodine retention has proven to be a valuable method for the early detection of iodine concentrating tissue in patients with thyroid cancer. The method is of particular interest to institutions without whole-body-counting facilities. It is obvious that the method with an uncollimated crystal (*2*) offers the advantage of a lower test dose. However, in a nuclear medicine department with changing background conditions, the use of collimation seems more reliable. In addition, the point-source response using the pinhole collimator shows better uniformity than with the open crystal.

ROBERT WILLVONSEDER
RUDOLF HÖFER
Department of Nuclear Medicine
2nd Medical Clinical
University of Vienna, Austria

FOOTNOTE

*Searle Radiographics Pho/gamma Scintillation Camera, Chicago, Ill.

REFERENCES

1. HARTMAN CR, HOFELDT FD, VERDON TA: The invalidity of ^{131}I urinary excretion studies in patients with thyroid carcinoma. *J Nucl Med* 13: 434, 1972

2. VERDON TA, MCCOWEN KD, HOFELDT FD: Use of the Anger scintillation camera for determining thyroid uptake. *J Nucl Med* 17: 359–361, 1976

3. HÖFER R, OGRIS E, VORMITTAG E, et al.: Verlaufsbeobachtungen speichernder metastasierender Schilddrüsencarcinome mit der Anger Kamera. In: 1. *Heidelberger Symposium über Kamera Szintigraphie*, Scheer KE, ed., 1969, pp 181–188

4. HÖFER R, WILLVONSEDER R: De l' utilité de la caméra a scintillations en tant qu' "anthropogammamètre" pour l'étude du cancer thyroïdien. *J Radiol Electrol* 51: 671–673, 1970

5. OBERHAUSEN E: Liquid scintillation whole body counters in: Clinical uses of whole body counting, Vienna, IAEA, 1966, pp 3–21

Reply

We thank Willvonseder and Höfer for their comments on our recent publication (*1*). We have read with interest the description of their technique using the scintillation camera as a whole-body counter. We agree with their comment that this method could be of great interest in institutions that do not have whole-body-counting facilities. In reply to their specific questions, we scheduled our patients during a slow period of the day (usually early morning) when background was at its lowest, since other patients were not being studied in the clinic at that time. We agree that a fluctuating background could be a major problem with this technique. Careful adherence to a prestudy background determination, shielding the patient from other patients in the clinic, and performing the procedure at "off times" seems to control this problem adequately. We also evaluated the pinhole collimator, but found that it took considerable time to obtain a reasonable number of counts. We therefore returned to using the uncollimated method as described in our article (*1*).

THOMAS A. VERDON, Jr.
Colorado Springs, Colorado

REFERENCE

1. VERDON TA, MCCOWEN KD, HOFELDT FD: Use of the Anger scintillation camera for determining thyroid uptake. *J Nucl Med* 17: 359–361, 1976

Quenching Curves

I would like to make comments regarding a number of inaccuracies in the paper by Barrows, Samols, and Becker (*1*).

First, in Fig. 1, the equations for efficiency should be read as follows: Eff. $= 99 - 75\chi + 30\chi^2$ for C-14 instead of Eff. $= 99 + 75\chi + 30\chi^2$; and Eff. $= 98 - 190\chi + 91\chi^2$ for H-3 instead of Eff. $= 98 + 190\chi + 91\chi^2$.

In Fig. 2, the equation for H-3 efficiency should read: Eff. $= -13.2 + 21.3\chi - 0.96\chi^2$ as opposed to Eff. $= 13.2 + 21.3\chi - 0.96\chi^2$.

Also, Table 1 has been amended.

TABLE 1. SAMPLE PRINTOUT FOR ALDOSTERONE RADIO IMMUNOASSAY

Tube	Channel A	Channel B	Corrected B	A/B	Efficiency (%)
1	17,114	43,847	116,292	0.3903	37.70
2	18,154	45,807	123,825	0.3963	36.99
3	18,393	46,417	125,450	0.3963	37.00
Averaged c.p.m.			121,855		
4	436	1,295	2,920	0.3367	44.35
5	367	1,068	2,457	0.3436	43.45
6	517	1,507	3,462	0.3431	43.52
Averaged c.p.m.			2,946		